Transactions, **SMiRT-26**
Berlin/Potsdam, Germany, July 10-15, 2022
Division V

DUCTILITY COEFFICIENT ASSESSMENT FOR RC WALLS AND SLABS SUBMITTED TO EXPERIMENTAL TESTS

Miquel Huguet[1], Philippe Bisch[2], Elias Bou-Said[2], Etienne Gallitre[3], Pierre-Yves Mertz[4], Philippe Merle[5], Rémi Meuzard[5]

[1] Civil Engineer, PhD, EGIS, Montreuil (France) (miquel.huguet-aguilera@egis.fr)
[2] Expert, EGIS, Montreuil (France)
[3] Expert, Gallitre Consultant, Verneiges (France)
[4] Civil Engineer, CSTB, Champs-sur-Marne (France)
[5] Civil Engineer, EDF, Lyon (France)

ABSTRACT

Reinforced Concrete (RC) structures submitted to relatively high-intensity seismic actions show a mechanical behaviour beyond the linear elastic domain. This phenomenon is at the origin of the ductility (absorbing displacements without major force softening) so of a capacity of energy dissipation that provides a seismic margin to the structure to resist the earthquake. This effect is expressed with the ductility coefficient F_μ that accounts for the reduction of the structural forces calculated with a linear elastic model. This work presents an experimental campaign on 8 RC walls and slabs representative of RC elements of nuclear power plants buildings. The experimental results are used to estimate their local ductility coefficients F_μ, using the "effective frequency/damping" method. The different possible choices of the elastic and admissible limit states and the obtained F_μ values are presented and commented.

INTRODUCTION

Reinforced Concrete (RC) structures submitted to relatively high-intensity seismic actions show a mechanical behaviour beyond the linear elastic domain, which is at the origin of the structure ductility (capacity to undergo displacements without major force softening). This capacity of energy dissipation contributes in earthquake resistance and increases the seismic margin. This effect is expressed with the ductility coefficient F_μ defined in the guide IAEA (2003) which accounts for the reduction of the structural forces calculated with a linear elastic model, which is the common engineering practice for performing structural analysis. For RC structures designed without seismic provisions, the ductility demand can be important if the constructive reinforcement arrangement of the structural elements are satisfactory. This work aims at estimating the F_μ values of RC walls and slabs representative of true structural elements in Nuclear Power Plant (NPP) buildings.

Let's consider the two different 1-D oscillators represented in the force-displacement curves of Figure 1. The first one is linear elastic and is characterised by its stiffness K (this oscillator could represent the engineering structural modelling). The second one is nonlinear and follows a bilinear force-displacement curve, where its elastic limit state is given by its elastic displacement δ_y and the elastic force or limit V_y (satisfying $K = V_y/\delta_y$) and its ultimate or admissible state is given by the ultimate displacement δ_u and the ultimate force V_u or capacity C. If we consider a seismic signal which brings the nonlinear oscillator to its admissible state (so that the ductility demand is maximum $\mu = \delta_u/\delta_y$), we can note V_{max} the maximum force of the linear oscillator during the seismic signal. Therefore, we define the ductility

coefficient F_μ as the reduction of the maximum force calculated using linear elastic assumptions with respect to a more-realistic bilinear force-displacement curve:

$$F_\mu = \frac{V_{max}}{V_y} \quad \tilde{F}_\mu = \frac{V_{max}}{C} \tag{1}$$

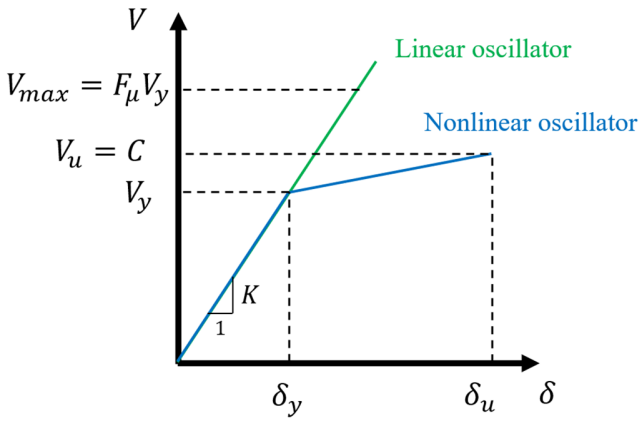

Figure 1. Characterisation of a bilinear force-displacement curve for the calculation of F_μ.

This paper is organised as follows. First, we present the experimental campaign consisting on 8 different tests on RC elements and we analyse some of the obtained results. Then, we present the "effective frequency/damping" method for calculating the ductility coefficient F_μ value depending on a number of assumptions and choices. Finally, this procedure is applied to the 8 tests of the experimental campaign and the obtained results are discussed.

THE EXPERIMENTAL CAMPAIGN

The 8 tests on RC walls and slabs

The experimental campaign has been performed by the CSTB at Champs-sur-Marne (France). The 8 tests concern mock-ups representing 3 different structural RC elements existing in NPP buildings which have been identified as critical in seismic situation using an elastic FE analysis:

- RC wall with vertical stiffeners at extremities, named M3
- RC wall, named M4
- RC slab, named M6

The typical test configuration is shown in Figure 2. The RC specimen is installed in a steel frame (the connection between them is assured by means of stiff top and bottom RC beams), from which the global in-plane shear force V and the tensile vertical load are applied. The vertical tensile force is applied using two hydraulic cylinders with a capacity of 600 kN. The transmission of the vertical force is ensured by two articulated lifting beams allowing the isostatic force to be applied at 16 points distributed over the top RC beam, which is connected by 16 chemical seals of M20 rods (with an anchorage depth of 60 mm). The horizontal force is applied with a cylinder with a stroke of 150mm and a capacity of 4500 kN, positioned at the centre of the top RC beam. It is linked to the steel frame via 2 HEB700 which are fixed using 8 prestressed bars.

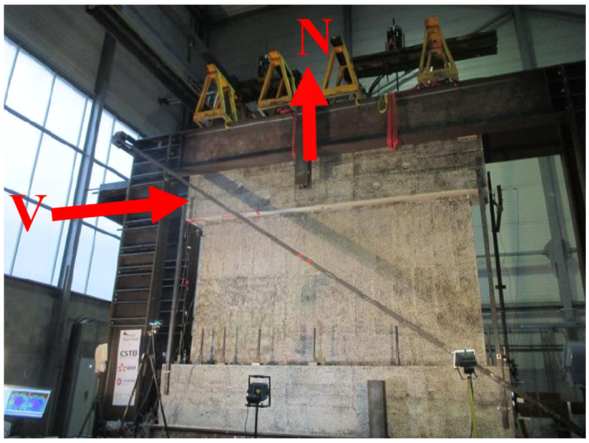

Figure 2. Example of test configuration (test 5: element M4 at geometrical scale 1) with the application of the tensile N and global shear V forces.

The specimens were manufactured in 2 steps. Firstly, the upper and lower RC beams and then, the central RC element. A metal plate at the top RC beam is welded with the steel structure in order to apply the mechanical loading.

Figure 3. Manufacturing steps.

The RC beam has vertical holes of ⌀=60 mm in order to connect the specimens to the steel frame via prestressed bars. The position of the holes is designed to take up the vertical lifting forces in relation to the frame mainly concentrated towards the zone where the external force is applied (located at the specimen extremity).

Table 1 presents the comparison between the 8 tests of the experimental campaign. The different parameters have been chosen in order to perform the sensibility analysis of:

- The mock-up geometrical scale: tests 2 and 5 are identical except for their geometrical scale (1/2 vs. 1)
- The reversing of the sign of the applied load: tests 5 and 8 are identical except for the type of cyclic load history (non-reversing vs. reversing)
- The contact conditions between the hydraulic actuator and the top RC beam: tests 1 and 7 are identical except for the friction condition (friction vs. sliding)
- The tensile vertical load: tests 3 and 4 are identical for element M3 and tests 3 and 4 for element M4, except for the tensile vertical load which is equal to 0 or to a representative value of the concomitant seismic tensile effort N so that the seismic efforts pair N-V is critical for the capacity of the element. These values are obtained from a linear elastic response spectrum structural analysis and the calculation of the in-plane bending, shear by diagonal cracking and sliding failure modes capacity for the 24 Newmark combinations. For these failure modes, the vertical force can increase (for compressive forces) or reduce (for tensile forces) the capacity. More details can be found in the *companion* paper Huguet et al. (2022).

Table 1: Comparison of the 8 tests of the experimental campaign

Test n°	Element	Type of element	Geometrical scale	Vertical tensile load (KN)	Reversing cyclic load	Contact between actuator and RC beam
1	M4	Wall	1/2	0	No	Friction
2	M4	Wall	1/2	175	No	Friction
3	M3	Wall+stiffners	1/2	250	No	Friction
4	M3	Wall+stiffners	1/2	0	No	Friction
5	M4	Wall	1	700	No	Sliding
6	M6	Slab	1	0	No	Sliding
7	M4	Wall	1/2	0	No	Sliding
8	M4	Wall	1	700	Yes	Sliding

Measurement device

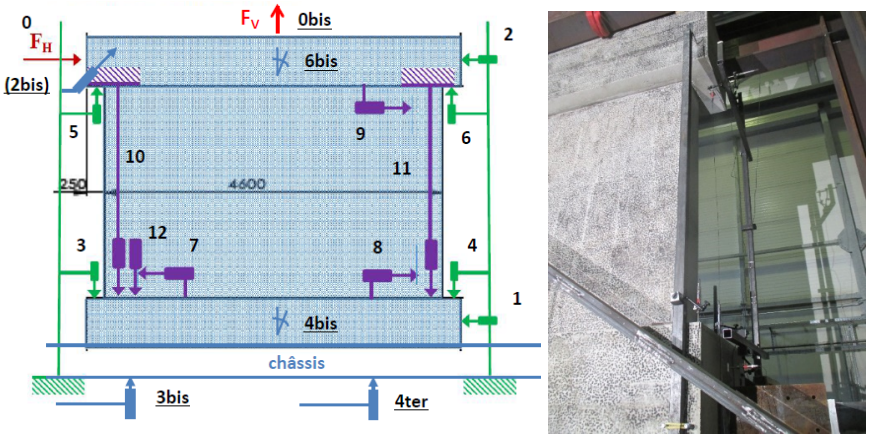

Figure 4. Measuring device.

The measurement device is composed by displacement sensors, strain gauges, inclinometers (see Figure 4) and a Digital Image Correlation (DIC) 3D full-field (see Figure 5 and Figure 6). This combination allows determining the displacements deformations in the entire RC specimen:

- the displacement sensors, inclinometers and the DIC analyse the external deformations,
- the strain gauges record the internal deformations of the steel reinforcement bars connecting the RC specimen with the RC beams.

Figure 5. DIC device.

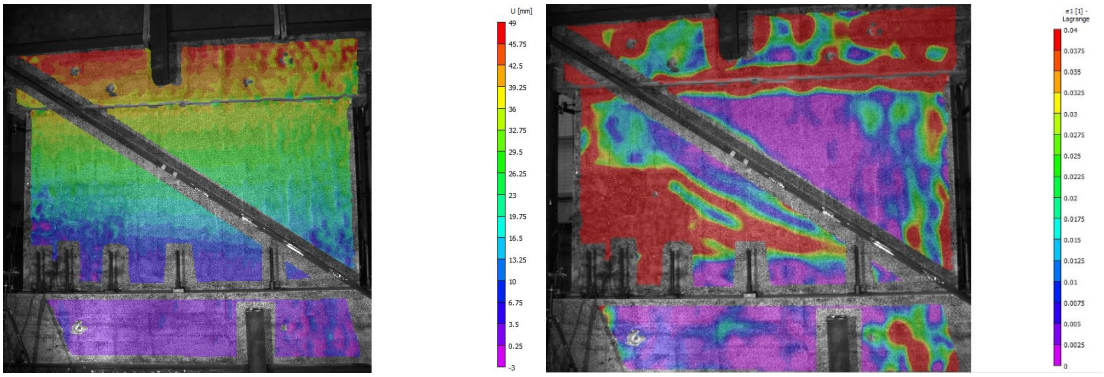

Figure 6. Displacement and strain measurements via DIC method.

THE EFFECTIVE FREQUENCY/DAMPING METHOD

The effective frequency/damping method proposed by NUREG (1984) and EPRI (1994) is based on the characterisation of the elastic secant oscillator equivalent to the nonlinear oscillator with the bilinear curve of Figure 1. The ultimate secant stiffness is defined by $K_s = V_u/\delta_u$ so its secant frequency is given by $f_s = f\sqrt{K_s/K}$, where f is the frequency of the linear oscillator. Then, the effective frequency f_e associated to the « average" non linear response during the earthquake is given by the weighted average:

$$f_e = (1 - A)\, f + A\, f_s \tag{2}$$

with $A = C_F(1 - f_s/f) \leq 0.85$. The value of the effective damping ratio β_e is obtained as the sum of the elastic β and hysteretic $\beta_H = C_N(1 - f_s/f)$ damping ratios, corrected by the effective frequency:

$$\beta_e = \left(\frac{f_s}{f_e}\right)^2 (\beta + \beta_H) \tag{3}$$

The coefficients C_F et C_N depend on the effective duration of the earthquake T_D and are given in Table 2.

Table 2: Values of C_F and C_N from NUREG (1984)

T_D (s)	C_F	C_N
<1	1,5	0,3
1-7	1,9	0,15
9-11	2,3	0,11
>15	2,7	0,11

Finally, the ductility coefficient F_μ can be calculated, for a given seismic input characterised by its elastic response spectrum in displacement $S_d(f,\beta)$ or in acceleration $S_a(f,\beta) = (2\pi f)^2 S_d(f,\beta)$, reads:

$$F_\mu = \mu_u \frac{S_d(f,\beta)}{S_d(f_e,\beta_e)} = \mu_u \left(\frac{f_e}{f}\right)^2 \frac{S_a(f,\beta)}{S_a(f_e,\beta_e)} \quad (4)$$

When this definition for an oscillator is applied for a particular structural member located in a larger structure, we deal with a *local* ductility coefficient. In this paper, we deal with this type of ductility coefficients. Huguet et al. (2022) present the calculation of *global* ductility coefficient of an entire structure. Therefore, we will consider that the frequency in Equation (4) is the one of the structure originating the critical efforts on the elements (provided by linear elastic analysis), so it supposes that the stiffness degradation of the entire structure is the same that the one of the element. This extreme assumption has implications in the application of Equation (4), since the ratio of the elastic response spectrum depends on the frequency relative position on the ascending, plateau or descending branches. From Huguet et al. (2019), the retained frequencies are in the ascending branch of the seismic response spectrum so the ratio $S_a(f,\beta)/S_a(f_e,\beta_e) > 1$. The obtained results provide higher F_μ values than those obtained for a representative frequency in the descending branch of the spectrum so $\frac{S_a(f,\beta)}{S_a(f_e,\beta_e)} < 1$.

APPLICATION TO THE 8 RC ELEMENTS OF THE EXPERIMENTAL CAMPAIGN

The procedure is based in a three-step procedure, which are detailed in the following sections:

1) Obtaining the representative envelop force-displacement curve
2) Idealisation of the envelop curve in a bilinear curve
3) Application of the effective frequency/damping method, presented in the previous chapter

1) Representative experimental force-displacement envelop curve

The first step consists in defining the representative force-displacement curve for reproducing the RC element mechanical behaviour. Actually, this step has two parts: (1) obtention of the force-displacement experimental curve and (2) determination of the envelop curve.

The experimental curves are defined by the global shear force V applied by the hydraulic actuator and the relative horizonal displacement (drift) between the top and the bottom RC beams (for some cases, corrected with the rigid body rotation of the element). The drift is calculated from experimental values from LVDT sensors, which has been compared and validated by comparison to the DIC results. Then, the envelop curve is obtained by neglecting the cycles and the local small non representative softening behaviours due to cycling. Figure 7 presents the obtained results. Two particular cases are commented here:

- Test n° 7: An instrumentation issue has not allowed to record the load and displacement at the first cycles. Therefore, here we propose two ways (propositions 1 and 3) to define the envelope curve corresponding to the first cycles by using test n°1 results (with and without normalisation of the curve). However, the conclusions obtained with the results of this test should be considered with caution.
- Test n° 8: This is the only alternate load history test and the "positive" and "negative" load directions are treated separately.

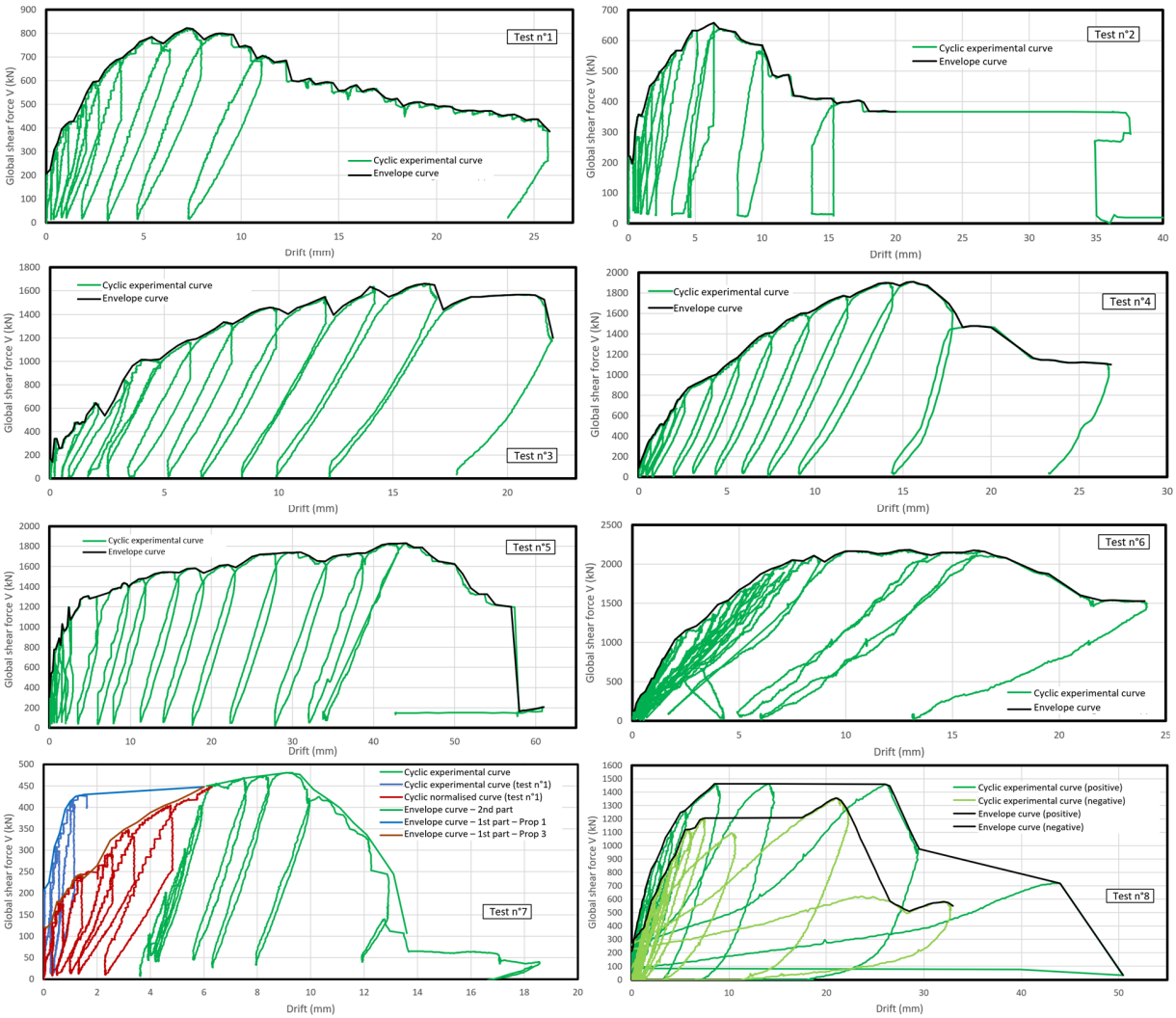

Figure 7. Experimental and retained envelop curves for the 8 tests.

2) Idealisation of a bilinear curve

The bilinear curves as the one of Figure 1 are defined by three points: origin (0,0), elastic limit (δ_y,V_y) and admissible limit (δ_u,V_u). The bilinear curves retained in this paper are shown in Figure 8:

1) Take the numerical elastic stiffness (with two assumptions for a sensibility analysis : cracked R and uncracked U concrete) of the element in the model used to the calculation of the modal analysis giving f, β for the linear elastic seismic analysis.

2) Take a point on the experimental envelop curve corresponding to the admissible limit. Four assumptions are considered : drift of 8‰ (A), 6‰ (B) et 4‰ (C), and the post-peak displacement giving an elastic – perfectly plastic curve (PP). The drift values of A, B and C limits are obtained from Table 5-2 of guide ASCE-SEI (2005).
3) With the previous conditions, define the elastic limit V_y so that the dissipated energy (are under the curve) of the bilinear idealised curve is equal to the one of the envelop experimental curve.

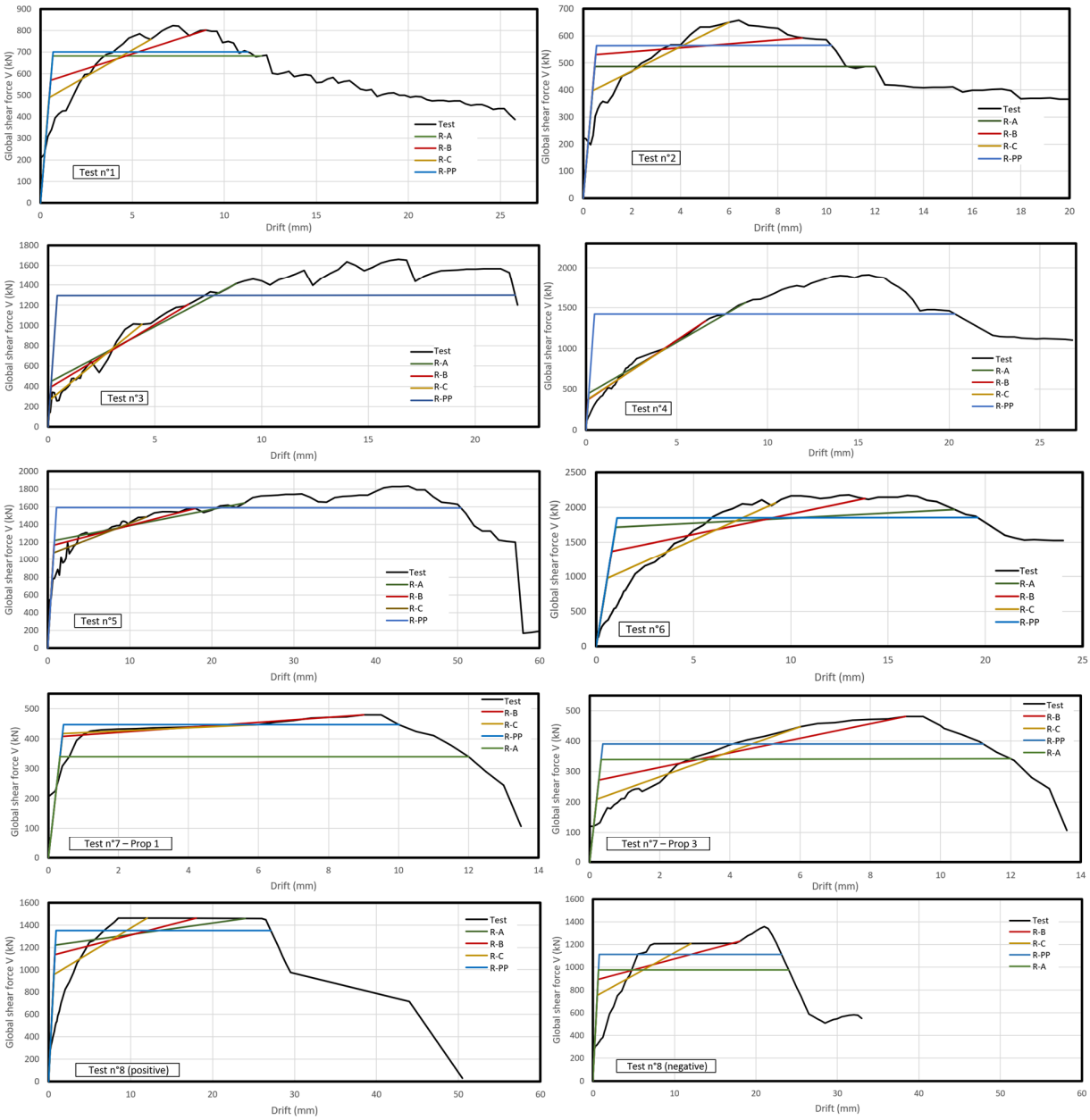

Figure 8. Experimental and retained envelop curves for the 8 tests.

3) Application of the effective ***frequency/damping method***

Finally, the "effective frequency/damping" method is applied to calculate the local F_μ ductility coefficients for the 8 RC specimens. Results of Table 3 show that, in general, the obtained values of the local F_μ ductility coefficients with Equation (4) are high. This is explained by two main reasons:

- The retained frequencies (associated to the main modes creating the highest structural efforts in the considered elements) are in the ascending branch of the seismic response spectrum so the ratio $S_a(f,\beta)/S_a(f_e,\beta_e) > 1$.
- The obtained experimental curves of Figure 7 show in general a large ductile behavior of the tested RC elements; therefore the calculated F_μ ductility coefficients are high since there are proportional to μ_u in Equation (4).

Table 3: Calculated values for the local F_μ ductility coefficient for the 8 experimental tests

Test n°	Drift 8‰ (A)		Drift 6‰ (B)		Drift 4‰ (C)		Post-peak (PP)	
	Uncracked	Cracked	Uncracked	Cracked	Uncracked	Cracked	Uncracked	Cracked
1	9,8	7,5	10,5	8,1	9,7	7,1	9,6	7,2
2	11,9	9,3	10,4	7,8	11,0	8,4	10,1	7,7
3	32,3	24,1	29,5	22,0	30,2	23,3	18,5	13,4
4	34,0	25,3	32,0	24,3	21,2	16,4	16,3	11,9
5	15,2	11,7	13,3	9,9	10,5	8,2	17,8	12,6
6	12,1	7,7	13,5	8,2	16,4	8,7	11,6	7,2
7-1	14,2	11,0	12,4	9,3	9,0	6,9	11,4	8,9
7-3	14,3	11,1	18,5	13,9	17,9	13,8	12,8	10,1
8+	14,3	11,0	13,2	9,9	11,9	9,2	12,9	10,1
8-	14,4	11,1	15,5	11,9	14,4	10,9	13,2	10,3

The comparison between the results presented in Table 3 for the different RC specimens allows assessing the effects of the variable parameters:

- Element M3 (RC wall with stiffeners) shows higher values of F_μ than element M4 (RC wall without stiffeners), since the elastic phase shown by M3 is relatively short, which implies high values of μ_u and F_μ.
- There is a relatively good correspondence between equivalent tests with different geometrical scale factors (comparison of results of tests 2 and 5), even if it decreases with the retained value of δ_u. This justifies the economic possibility of using reduced scale specimens.
- There is no clear trend of the effect of the inversion of the sign of the applied load history (comparison of tests 5 and 8), except for a decrease of F_μ for the alternate load for PP curve (associated to large ductility values).
- The value of F_μ increases when there is free sliding between the hydraulic actuator and the top RC beam (test 7) since the adherence in test 1 creates a more relative fragile force peak.
- There is no clear trend of the effect of the application of the vertical tensile load, which is assessed by comparing the results of tests 2 and 3 with those of tests 1 and 4, respectively.

CONCLUSION

The experimental campaign concerning mechanical tests on 8 RC walls and slabs representing 3 different RC elements of a NPP building has been challenging. The comparison between LVDT and DIC displacement sensors have shown good results. The obtained force-displacement curves are different for each tested element and each sensibility analysis concerning the geometrical scale, the type of applied load history, the concomitance of vertical tensile load and the adherence conditions between the force actuator and the top RC beam.

This paper presents an operative method (consisting in three steps) to assess the local F_μ ductility coefficient from experimental results, which uses the "effective frequency/damping" method defined by NUREG (1985). When the ductility coefficients are used in accordance to a structural analysis, it is important to take the numerical stiffness of the element giving the retained value of the representative frequency. Also, the ductility and ductility coefficients values depend in the definition of admissible state; here 4 different possible definitions are considered. The obtained results show high values of F_μ mainly originated by (i) the high values of μ_u in the idealised bilinear curves and the row force-displacement experimental curves, and (ii) the structural frequencies creating the main efforts in the considered RC elements which are in the ascending branch of the seismic response spectrum so the ratio $S_a(f,\beta)/S_a(f_e,\beta_e) > 1$. We observe little dependence on the geometrical scale, the reversing of the applied shear load and the concomitant tensile force; only the effect of a free sliding force actuator is relevant as it allows a more ductile behaviour.

REFERENCES

ASCE/SEI, 43-05, Seismic Design Criteria for Structures, Systems and Components in Nuclear Facilities, 2005

EPRI (1994), TR-103959 Research Project – *Methodology for Developing Seismic Fragilities*.

Huguet, M., Erlicher, S., Bou-Said, E., Bisch, P., Gallitre, E., Courtois, A. (2022). "Ductility coefficient assessment for RC walls and slabs submitted to experimental tests", *Proc., SMiRT 26*, IASMiRT, Berlin

Huguet, M., de Mersseman, J., Bou Said, E., Erlicher, S., Bisch, P., Gallitre, E. (2019). "Projet MAESTRO : Estimation des coefficients de ductilité de voiles et planchers en béton armé à partir d'essais expérimentaux", *Proc. 10ème Colloque National de l'AFPS*, Strasbourg, France.

IAEA (2003). *Safety Reports Series No.28 – Seismic Evaluation of Existing Nuclear Power Plants*

NUREG (1984). CR-3805 – *Engineering Characterization Of Ground Motion – Task II Vol.2 - Effects of Ground Motion Characteristics on Structural Response Considering Localized Structural Nonlinearities and Soil-Structure interaction Effects.*